Density of states for a dielectric superlattice. II. TM polarization

Jorge R. Zurita-Sánchez and P. Halevi
Instituto Nacional de Astrofísica Óptica y Electrónica, Apartado Postal 51, Puebla, Puebla 72000, Mexico
(Received 14 June 1999)

We present an analysis of the band structure, the equifrequency surfaces, and the density of states (DOS) for the transverse magnetic (TM) polarization mode of the dielectric superlattice, modeled by means of Dirac-delta functions. This complements a recent article [Phys. Rev E **59**, 3624 (1999)] that analyzes the case of transverse electric (TE) polarization. Unfortunately, for this simple model, there is no manifestation of the Brewster effect in the band structure for the TM modes. For large values of the frequency or the grating strength, the equifrequency surfaces essentially degenerate into a set of concentric, hollow, and narrow cylinders centered on the superlattice axis. The DOS is enhanced relative to free space for any frequency and it exhibits discontinuities in the slope at the band edges. These results are relevant to the spontaneous emission by an atom or to dipole radiation in one-dimensional periodic structures. The differences between TE and TM modes are discussed. We take the opportunity to correct an error in the DOS calculation for TE polarization in the article referred above.

PACS number(s): 42.70.Qs, 42.25.Bs, 78.20.Bh

I. INTRODUCTION

Recently the transverse electric (TE) polarization modes were calculated for an idealized model of a dielectric superlattice (SL) [1]. This ''Dirac-comb'' model is defined by means of a one-dimensional, periodic distribution of Dirac delta functions in a background dielectric medium [2], and yields a band structure that is similar to that obtained from the realistic model of the SL [3]. In this work, here referred to as paper I, the surfaces of constant frequency [$\omega(\mathbf{k})=\text{const}$] and the density of modes, or density of states (DOS), were also plotted for the TE modes.

The present paper is closely related to paper I; it concerns the very same, ''Dirac-comb'' model of the SL, now, however, we study the transverse magnetic (TM) modes (Sec. II), thus completing the investigation of the normal modes of this system. In Sec. III we present the calculation of the DOS using the equifrequency surfaces. In Sec. IV we take the chance to correct an error in the calculation of the DOS of the TE modes in paper I. The conclusions are presented in Sec. V, although the differences between the TE and TM modes are discussed throughout the paper.

We complement the list of references in paper I with four papers by Scalora and associates [4–7]. They are all restricted to propagation parallel to the SL axis, and mostly deal with pulse transmission in structures with a finite number of periods. Specifically, in Ref. [5] analytic expressions are found for the DOS in terms of the complex transmission coefficient.

II. NORMAL MODES

A. The Dirac-delta model

We consider an inhomogeneous, linear, and nonmagnetic medium in which the Dirac-delta model is used to represent the dielectric constant dependence on the position, i.e.,

$$\epsilon(x)=\epsilon_o+gd\sum_{n=-\infty}^{\infty}\delta(x-nd). \tag{1}$$

Here the g parameter is called the *grating strength*, d is the period of the dielectric function, and ϵ_o is a background dielectric constant. As a brief explanation of this ''Dirac-comb'' model, we can say that it comes from considering a real SL, formed by an infinite array of alternating layers with dielectric constants ϵ_o and ϵ_m whose widths are $d-\Delta$ and Δ, respectively (see Fig. 1 of paper I), and d is the period. If we take the limits $\epsilon_m\to\infty$ and $\Delta\to 0$ in such a way that the factor $\epsilon_m\Delta/d$ is kept constant, then the Dirac-delta model can be obtained (see paper I). In this limit the factor $\epsilon_m\Delta/d$ becomes the grating strength g that appears in Eq. (1).

B. TM modes

In an inhomogeneous dielectric medium, Maxwell's equations lead to the following wave equation for the magnetic induction field $\mathbf{B}(\mathbf{r})$:

$$\nabla^2\mathbf{B}(\mathbf{r})+\frac{\nabla\epsilon(\mathbf{r})}{\epsilon(\mathbf{r})}\times[\nabla\times\mathbf{B}(\mathbf{r})]+\frac{\omega^2\epsilon(\mathbf{r})}{c^2}\mathbf{B}(\mathbf{r})=\mathbf{0}. \tag{2}$$

Here ω is the frequency of the monochromatic field. Since the dielectric constant function, Eq. (1), depends only on x, for the TM polarization the magnetic induction $\mathbf{B}$ lies in the yz plane. Therefore it must have the functional form

$$\mathbf{B}_\mathbf{k}(x,y,z)=B_\mathbf{k}(x)e^{i(k_y y+k_z z)}\hat{\mathbf{e}}_\mathbf{k}, \tag{3}$$

where $\hat{\mathbf{e}}_\mathbf{k}$ is an arbitrary unit vector in the yz plane. Substituting Eq. (3) into Eq. (2), we obtain

$$\frac{d^2B_\mathbf{k}(x)}{dx^2}-\frac{1}{\epsilon(x)}\frac{d\epsilon(x)}{dx}\frac{dB_\mathbf{k}(x)}{dx}+B_\mathbf{k}(x)\left[\frac{\omega_\mathbf{k}^2}{c^2}\epsilon(x)-k_y^2-k_z^2\right]=0. \tag{4}$$

Within the regions between the barriers $\epsilon(x)=\epsilon_0=\text{const}$, so the second term of Eq. (4) vanishes. Then the solution for $B_\mathbf{k}(x)$ is of the form

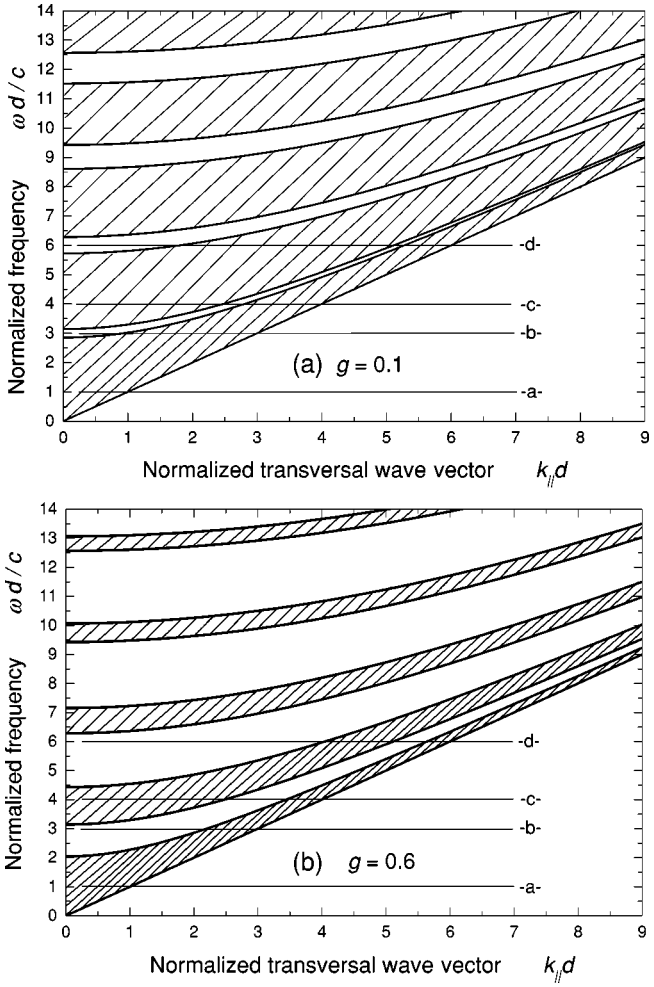

FIG. 1. Band structure for the Dirac-delta model superlattice, obtained by using the dispersion relation Eq. (17) for $\epsilon_o=1$, (a) $g=0.1$ and (b) $g=0.6$. The widths of the forbidden bands increase with g; the upper band edges move downward, while the lower band edges are fixed at $\omega d/c=\pi n$ ($n=0,1,\ldots$) on the frequency axis. The free-space dispersion relation is recovered in the limit $g\to 0$, namely, the band gaps shrink to zero.

$$B_{\mathbf{k}}^{(n)}(x)=A_n e^{iK(x-nd)}+B_n e^{-iK(x-nd)},$$

$$(n-1)d<x<nd, \tag{5}$$

$$n=0,\pm 1,\pm 2,\ldots .$$

Here K is given by

$$K=\sqrt{\frac{\omega_{\mathbf{k}}^2}{c^2}\epsilon_o-k_\parallel^2}, \tag{6}$$

and $k_\parallel$ is magnitude of the projection of the wavevector $\mathbf{k}$ on the yz plane, i.e., $k_\parallel^2=k_y^2+k_z^2$. Using the Bloch theorem it is possible to obtain $B_{\mathbf{k}}$ in the n^{th} region in terms of the region $n=0$, that is,

$$B_{\mathbf{k}}^{(n)}(x)=e^{ik_B nd}[A_o e^{iK(x-nd)}+B_o e^{-iK(x-nd)}],$$

$$(n-1)d<x<nd, \tag{7}$$

$$n=0,\pm 1,\pm 2\ldots .$$

Here k_B is the Bloch wavevector, defined in the first Brillouin zone ($-\pi/d<k_B\leqslant\pi/d$). We tried to apply the same methodology used in I for the TE polarization in order to derive the boundary conditions at the ''barriers'' $x=nd$. That is, we integrated Eq. (4) over a very small interval around the barriers. Unfortunately, due to the strong singularity of the dielectric constant function $\epsilon(x)$ at the barriers, this procedure failed. Instead, we use another approach, namely, we solve the eigenvalue problem for the model of Eq. (1) as a limit of the real SL.

C. Solution of the eigenvalue problem; the band structure

First, consider a real SL as the one described at the end of Sec. II A. For this case, the coefficients for the solution of the field $B_{\mathbf{k}}^{(n)}(x)$ in two regions with dielectric constant ϵ_o separated by a region with dielectric constant ϵ_m, are related by [3]

$$\begin{pmatrix} A_{n-1} \\ B_{n-1} \end{pmatrix}=\begin{pmatrix} f_1 & f_2 \\ f_2^* & f_1^* \end{pmatrix}\begin{pmatrix} A_n \\ B_n \end{pmatrix}, \tag{8}$$

$$f_1=e^{-iK(d-\Delta)}\left[\cos(K_m\Delta)-\frac{i}{2}\left(\frac{K_m\epsilon_o}{K\epsilon_m}+\frac{K\epsilon_m}{K_m\epsilon_o}\right)\sin(K_m\Delta)\right], \tag{9}$$

$$f_2=-\frac{i}{2}e^{iK(d-\Delta)}\left[\frac{K_m\epsilon_o}{K\epsilon_m}-\frac{K\epsilon_m}{K_m\epsilon_o}\right]\sin(K_m\Delta), \tag{10}$$

$$K_m=\sqrt{\frac{\omega^2}{c^2}\epsilon_m-k_\parallel^2}. \tag{11}$$

Now we apply the following limits [2] to the matrix elements Eqs. (9) and (10):

$$\Delta\to 0,\quad \epsilon_m\to\infty,$$

$$\sqrt{\epsilon_m}\Delta\to 0,\quad \epsilon_m\Delta\to gd=\text{const.}$$

Then Eqs. (9) and (10) simplify to

$$f_1=e^{-iKd}[1-i\alpha(K)], \tag{12}$$

$$f_2=i\alpha(K)e^{iKd}, \tag{13}$$

$$\alpha(K)\equiv\frac{gd}{2\epsilon_o}K. \tag{14}$$

Now, from Eqs. (5) and (7)

$$\begin{pmatrix} A_n \\ B_n \end{pmatrix}=e^{ik_B d}\begin{pmatrix} A_{n-1} \\ B_{n-1} \end{pmatrix}. \tag{15}$$

Then combining the Eqs. (8) and (15) the characteristic matrix $\mathbf{M}$ is obtained

$$\mathbf{M}\begin{pmatrix} A_n \\ B_n \end{pmatrix} \equiv \begin{pmatrix} f_1 - e^{-ik_B d} & f_2 \\ f_2^* & f_1^* - e^{-ik_B d} \end{pmatrix} \begin{pmatrix} A_n \\ B_n \end{pmatrix} = \mathbf{0}. \quad (16)$$

In order to have nontrivial solutions, the determinant of **M** must be zero. Then we obtain that

$$\cos(k_B d) = \cos(Kd) - \alpha(K)\sin(Kd). \quad (17)$$

Equation (17) is the desired dispersion relation. It is formally the same as the dispersion relation Eq. (19) of paper I for the TE modes. The difference is entirely due to the fact that, for TE modes, $\alpha(K) = gd\omega^2/(2c^2K)$. In the present case, α depends on ω only implicitly, through K, and this will affect qualitatively the DOS.

In Fig. 1 we plot the band structure for $g = 0.1$ and $g = 0.6$. The shadowed regions are the allowed bands. It is known [8] that the lower and upper edges of the first band are characterized by $k_B = 0$ and $k_B = \pm \pi/d$, respectively. The order is inverted for the second band, namely, its lower and upper edges are given, respectively, by $k_B = \pm \pi/d$ and $k_B = 0$. For the third band the corresponding values are $k_B = 0$ and $k_B = \pm \pi/d$, and so on for the other bands. Thus all the band edges are characterized by $\cos(k_B d) = \pm 1$. For these values of the left side of eq. (17) there is one simple solution, namely $Kd = \pi n$, where $n = 0, \pm 1, \pm 2, \ldots$. Using Eq. (11) this gives

$$\frac{\omega^2}{c^2}\epsilon_o = \frac{\pi^2}{d^2}n^2 + k_\parallel^2. \quad (18)$$

It follows that the lower band edges are independent of g [see Figs. 1(a) and 1(b)]. For $k_\parallel = 0$ we have $\omega d/c = (\pi\sqrt{\epsilon_o})n$, which, we see from Fig. 1, gives the intercepts of the lower band edges on the frequency axis. In the asymptotic limit $\omega/k \to c/\sqrt{\epsilon_o}$, which is the speed of light in the background medium between the barriers. It is interesting that for $n = 0$ we also obtain $\omega/k = c/\sqrt{\epsilon_o}$, which is to say that the lower edge of the first band is a straight line. Then, glancing at Fig. 1, it is apparent that always $\omega/k > c/\sqrt{\epsilon_o}$. It follows from Eq. (11) that K can never be imaginary—unlike the case of TE polarization.

Equation (18) is valid for TE, as well as for TM modes, except for $n = 0$. In the case of the lowest ($n = 0$) TE band, $K = 0$ is *not* a solution for $k_B = 0$ because α is inversely proportional to K [hence the second term in Eq. (19) of paper I does not vanish]. Therefore, the lowest band edge is not a straight line in case of TE polarization.

It is not possible to derive an explicit formula for the upper band edges, and Eq. (17) must be solved numerically. These bands are displaced downward as the g parameter increases, so the forbidden bandgaps get wider, as is seen by comparing the Figs. 1(a) and 1(b). In fact, we notice from Fig. 1 that the band structure is very sensitive to the g parameter.

The *realistic* model of the superlattice predicts a distinctive feature for the TM modes, namely, the closure of the band gaps alongside a straight line through the origin in the ω/c versus $k_\parallel$ diagram [3] because of the Brewster's condition. The slope of this line is $\sqrt{1/\epsilon_m + 1/\epsilon_o}$. In the limit $\epsilon_m \to \infty$ this reduces to $1/\sqrt{\epsilon_o}$, which just coincides with the lower edge of the first band. It is then clear that our ''Dirac-comb'' model cannot give rise to the Brewster effect and, indeed, no closure of the bandgaps is manifest in Fig. 1.

Next we turn to the determination of the eigenvectors, namely, $B_{\mathbf{k}}^{(n)}(x)$. Using Eq. (16) the coefficients A_o and B_o are related by

$$B_o = \frac{e^{-ik_B d} - f_1}{f_2} A_o, \quad (19)$$

so, $B_{\mathbf{k}}^{(n)}(x)$ from Eqs. (19) and (7) can be expressed as

$$B_{\mathbf{k}}^{(n)}(x) = A_o e^{ik_B dn}\left\{ e^{iK(x-nd)} + \frac{i}{\alpha}[(1 - i\alpha)e^{-2iKd} - e^{-i(k_B+K)d}]e^{-iK(x-nd)} \right\}. \quad (20)$$

III. DENSITY OF STATES

We obtain the DOS $D(\omega)$ from Eq. (25) of paper I, which is independent of the polarization

$$D(\omega) = \frac{V}{4\pi^2}\int_{\omega_{\mathbf{k}}} \frac{k_\parallel}{|\nabla_{\mathbf{k}}\omega|} d\kappa_t. \quad (21)$$

The integration is carried out on the curve formed by the intersection of an *equifrequency* surface [$\omega(\mathbf{k}) = \text{const}$] with the $k_B k_y$ (or $k_z = 0$) plane, and $d\kappa_t$ is a differential segment of this curve. The equifrequency surfaces are formed by rotating these curves around the k_B axis. In Fig. 2 we display the curves obtained from the intersection of the equifrequency surfaces with the $k_B k_y$ plane for several normalized frequency ($\omega d/c$) values and for $g = 0.1$ and $g = 0.6$. The horizontal lines that appear in Fig. 1 represent the chosen frequency values for the Fig. 2 plots. The line (a) is entirely in the first allowed band, consequently the equifrequency curve is closed. In the limit $g \to 0$, the equifrequency surface is the sphere $k_B^2 + k_y^2 + k_z^2 = \omega^2\epsilon_o/c^2$, as it should be. As g increases the ''ellipse's'' eccentricity increases. Part of line (b) lies in the first forbidden band gap and the other part in the first allowed band; therefore the equifrequency surface is interrupted in the region where the solution for the field does not exist. The lines (c) and (d) represent more complex plots since they cross several forbidden and allowed bands. Also, we can notice that for a given frequency, the equifrequency curves for different values of g are tangent to each other at $k_B = 0$ and at $k_B d = \pm \pi$. This can be understood from the fact that Eq. (18), for the lower band edges, is independent of g. For comparison, in Fig. 2 we also show the equifrequency surfaces for the TE polarization mode, with $g = 0.6$ (dotted line). We call attention to the fact that, for higher values of ω or g, these plots tend to become elongated in direction of k_B. This occurs for both modes, but more so for the TE polarization. The meaning of this feature is that, for large frequencies or grating strength (or dielectric contrast, in the case of a real SL), the equifrequency surfaces essentially become a set of concentric, hollow, and narrow circular cylinders; see Fig. 2(d), $g = 0.6$. Of course, the explanation is that, the greater ω or g are, the wider the band gaps become, thus narrowing down the values of $k_\parallel$ allowed for propagation.

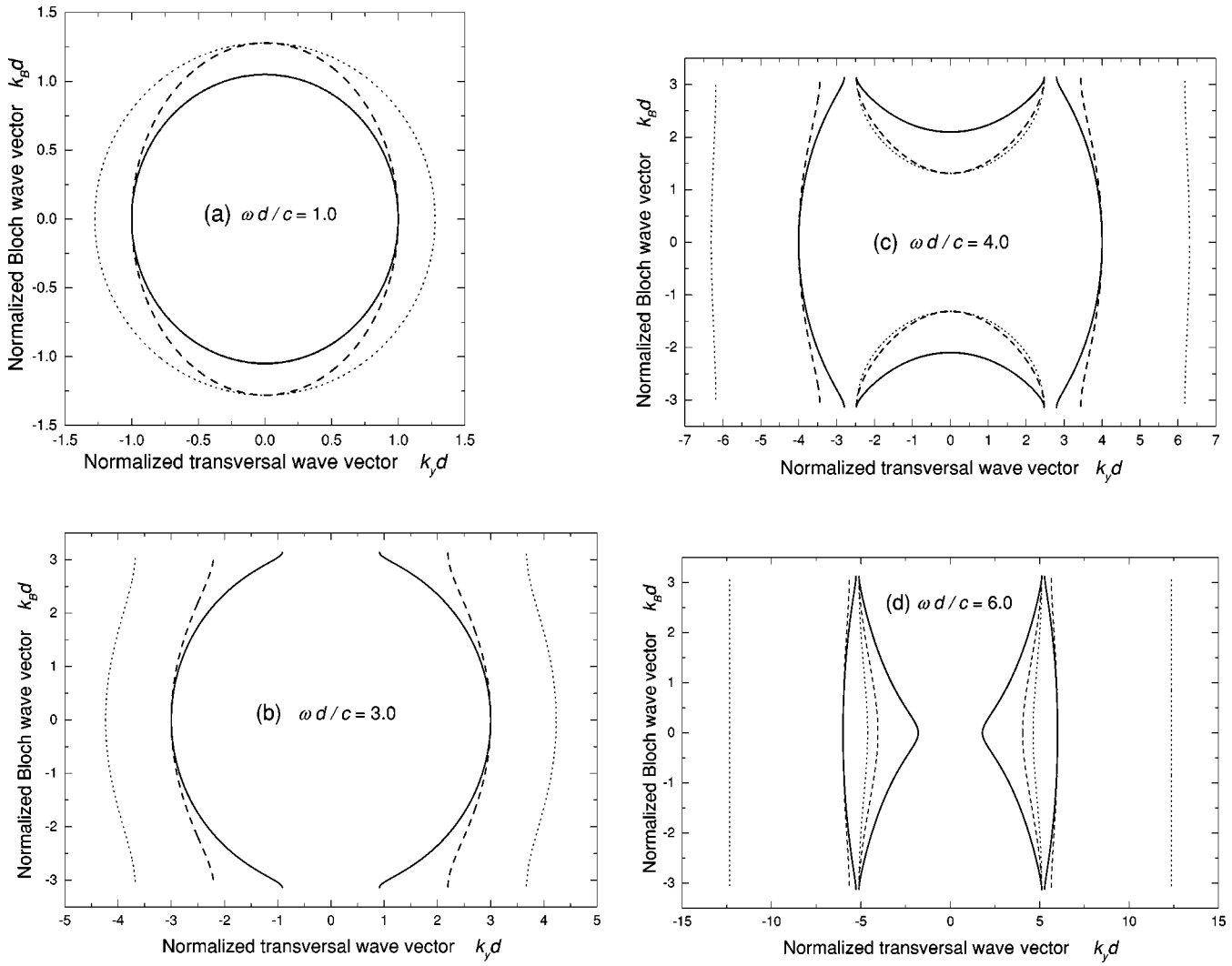

FIG. 2. Four intersections of normalized equifrequency surfaces $\omega(k_B,k_y,k_z)d/c=\text{const}$ with the normalized k_Bd-k_yd plane for TM and TE modes. The solid lines and the dashed lines correspond to TM modes for $g=0.1$ and $g=0.6$, respectively. The dotted lines correspond to TE modes for $g=0.6$, and are plotted for comparison. (a) Normalized equifrequency surface for $\omega d/c=1.0$. (b) For $\omega d/c=3.0$ the curves are interrupted because there is no propagating solution for this region of $k_\parallel$ values; see Fig. 1, line b. (c) For $\omega d/c=4.0$. (d) For $\omega d/c=6.0$ there are two interrupted regions, as can be understood from Fig. 1, line d.

The gradient of the frequency ω with respect to wave vector $\mathbf{k}$ is given by

$$\nabla_{\mathbf{k}}\omega=\frac{\partial\omega}{\partial k_B}\hat{\mathbf{x}}+\frac{\partial\omega}{\partial k_y}\hat{\mathbf{y}}+\frac{\partial\omega}{\partial k_z}\hat{\mathbf{z}}. \tag{22}$$

Using the Eqs. (11) and (17), Eq. (22) becomes

$$\nabla_{\mathbf{k}}\omega=\frac{c^2}{\epsilon_0\omega}\left[\frac{K\sin(k_Bd)}{F[K(\omega,k_\parallel)]}\hat{\mathbf{x}}+k_y\hat{\mathbf{y}}+k_z\hat{\mathbf{z}}\right]. \tag{23}$$

Here the function $F[K(\omega,k_\parallel)]$ is defined as

$$F[K(\omega,k_\parallel)]\equiv\sin(Kd)\left(1+\frac{g}{2\epsilon_0}\right)+\frac{g}{2\epsilon_o}Kd\cos(Kd). \tag{24}$$

Finally, substituting Eq. (23) into Eq. (21) the DOS for TM polarization is obtained as

$$D(\omega)=\frac{V\epsilon_o\omega}{4\pi^2c^2}\int_{\omega_{\mathbf{k}}}\frac{k_\parallel|F[K(\omega,k_\parallel)]|}{\sqrt{K^2\sin^2(k_Bd)+\{k_\parallel F[K(\omega,k_\parallel)]\}^2}}d\kappa_t. \tag{25}$$

The DOS function vs normalized frequency $\omega d/c$ for several values of g is shown in Fig. 3. The discontinuities of the slopes occur at the frequency band gap edges for $k_\parallel=0$ [compare with the intercepts $\omega(k_\parallel=0)$ in Fig. 1 for $g=0.1$ and $g=0.6$]. When the frequency reaches a lower band gap edge the slope of the DOS function is abruptly diminished. On the contrary, when it reaches the upper bandgap edge the slope suddenly increases. For these latter frequency values, given by $\omega d/c=(\pi/\sqrt{\epsilon_o})n$ according to Eq. (18), the DOS coincides with the free space DOS (dashed curve). This feature is not exhibited by the TE polarization, as we will see in next section. The DOS never vanishes and, for any frequency ω, it is never smaller than that of free space.

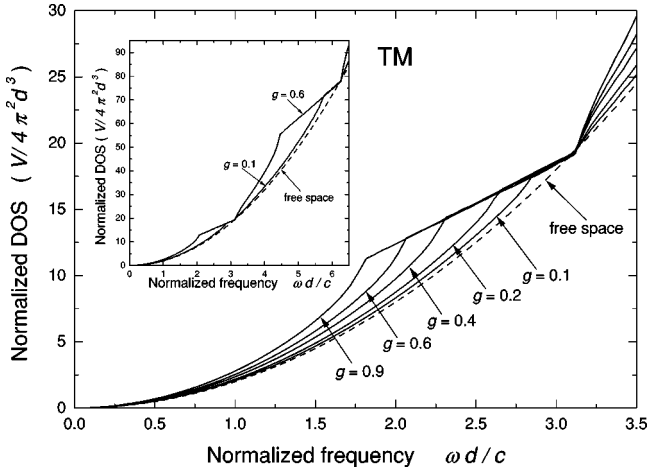

FIG. 3. Normalized density of states $[D(\omega d/c) = dN/d(\omega d/c)]$ for TM polarization as a function of the normalized frequency $\omega d/c$, for several values of g. The inset extends the frequency range to the interval $(0,2\pi)$. Note the discontinuities in the slope for frequencies that define the band gap edges. Notice, the DOS is enhanced for all values of ω and g with respect of that of free space.

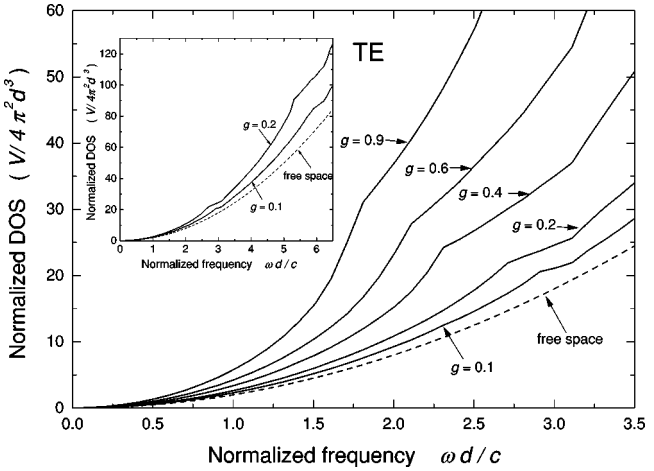

FIG. 4. Normalized density of states $[D(\omega d/c) = dN/d(\omega d/c)]$ for TE polarization as a function of the normalized frequency $\omega d/c$ for several values of the grating strength g. The inset extends the frequency range to the interval $(0,2\pi)$. We can see the discontinuities in the slope for frequencies that define the band-gap edges. (The plot is a bit ''wavy'' for the normalized frequency values close to 2π because of computational difficulties.) Notice that the DOS is enhanced for all values of ω and g. This figure replaces the erroneous Fig. 5 of paper I.

IV. COMPARISON WITH THE DOS FOR THE TE POLARIZATION

We take the opportunity to correct an error in paper I, specifically in the calculation of the y and z components of the gradient of ω with respect to $\mathbf{k}$ [Eq. (26) of paper I]. Equations (27) and (28) of paper I should be replaced by

$$|\nabla_{\mathbf{k}}\omega|_{\mathrm{TE}} = \frac{c^2}{\omega\epsilon_o}\left|\frac{1}{F(\omega,K(\omega,k_\parallel))}\left\{K\sin k_B d\,\hat{\mathbf{x}} + \left\{F[\omega,K(\omega,k_\parallel)] - \frac{g}{\epsilon_o}\sin Kd\right\}(k_y\hat{\mathbf{y}} + k_z\hat{\mathbf{z}})\right\}\right|,$$

$$D(\omega)_{\mathrm{TE}} = \frac{V\epsilon_o\omega}{4\pi^2c^2}\int_{\omega_{\mathbf{k}}} d\kappa_t \times \frac{k_\parallel|F[\omega,K(\omega,k_\parallel)]|}{\sqrt{K^2\sin^2 k_B d + k_\parallel^2\left\{F[\omega,K(\omega,k_\parallel)] - (g/\epsilon_o)\sin Kd\right\}^2}},$$

where the function $F[\omega,K(\omega,k_\parallel)]$ is defined by Eq. (29) of paper I.

The corrected Density of States (DOS) plot obtained from Eq. (28), for several values of g, is shown in Fig. 4. In comparison to the original figure (Fig. 5 of paper I), some qualitative features remain the same: the discontinuities of the slopes of the curves occur at the band gap edges, and there is an enhancement of the DOS with respect to that of free space. The differences are that the sharp peaks at the lower edges of the gaps are absent and that curves for different values of g never cross.

V. CONCLUSIONS

Using the ''Dirac-comb'' model of a SL, we have derived the band structure for the TM modes. The lower band edges are given by a simple, explicit formula and they do not depend on the grating strength g. This is also valid for the TE modes except for the lowest band edge. The lowest band edge is a straight line of slope $\omega/k_\parallel = c/\sqrt{\epsilon_o}$ for TM modes; not so for TE modes. We have also plotted the equifrequency surfaces. For large values of ω or g, they become, essentially, a set of concentric, hollow, and narrow circular cylinders centered on the SL axis. For the TM polarization, no reduction of the DOS occurs for any frequency with respect to that of free space. The DOS is an increasing function of the frequency, and it has slope discontinuities at the band edges. At the upper band edges the slope diminishes abruptly, then at the lower band edges it abruptly increases. These characteristics are also present for the TE polarization. However, the DOS plots for TM modes, for different values of g join at the upper band edges, while, in comparison, those for the TE modes never cross.

Even though the widths of the forbidden band gaps can be adjusted with g, this ''Dirac-comb'' model for the TM polarization has the disadvantage that the Brewster effect is not manifest. Therefore, some qualitative features of the DOS of the TM modes for the real SL, in comparison to those of this simplified model, could be different. On the other hand, for the TE polarization the parameter g, can be adjusted to give qualitative insight into optical properties of the real SL for this polarization. We expect these results for the DOS to be relevant for the analysis of spontaneous emission in superlattices.

ACKNOWLEDGMENTS

J.R.Z. thanks CONACyT and Sistema Nacional de Investigadores for financial support.

[1] I. Alvarado-Rodríguez, P. Halevi, and J.J. Sánchez-Mondragon, Phys. Rev. E **59**, 3624 (1999).
[2] J.P. Dowling and C.M. Bowden, Phys. Rev. A **46**, 612 (1992).
[3] A. Yariv and P. Yeh, *Optical Waves in Crystals* (Wiley, New York, 1984), Chap. 6.
[4] Michael Scalora, Jonathan P. Dowling, Aaron S. Manka, Charles M. Bowden, and Joseph W. Haus, Phys. Rev. A **52**, 726 (1995).
[5] Jon M. Bendickson, Jonathan P. Dowling, and M. Scalora, Phys. Rev. E **53**, 4107 (1996).
[6] M. Scalora, R.J. Flynn, S.B. Reinhardt, R.L. Fork, M.J. Bloemer, M.D. Tocci, C.M. Bowden, H.S. Ledbetter, J.M. Bendickson, J.P. Dowling, and R.P. Leavitt, Phys. Rev. E **54**, R1078 (1996).
[7] M. Scalora, M.J. Bloemer, A.S. Manka, J.P. Dowling, C.M. Bowden, R. Viswanathan, and J.W. Haus, Phys. Rev. A **56**, 3166 (1997).
[8] C. Kittel, *Introduction to Solid State Physics*, 7th ed. (Wiley, New York, 1996).